11th International Conference on Vibration Problems
Z. Dimitrovová *et al.* (eds.)
Lisbon, Portugal, 9-12 September 2013

THE INFLUENCE OF AXIAL LOADS ON THE DYNAMIC INSTABILITY OF CRUCIFORM COLUMNS WITH LOW TORSIONAL STIFFNESS

Carvalho E.C.*[1], Gonçalves P.B.[1], Rega G.[2], Del Prado Z.J.G.N.[3]

[1]Pontifical Catholic University, Rio de Janeiro, RJ, Brazil
eulher@tecgraf.puc-rio.br, paulo@puc-rio.br

[2]Sapienza University of Rome, Rome, Italy
giuseppe.rega@uniroma1.it

[3]Federal University of Goiás, Goiânia, GO, Brazil
zenon@eec.ufg.br

Keywords: Nonlinear Vibrations, Dynamic Instability, Flexural-Flexural-Torsional Coupling, Effect of Axial Static Preload, Bifurcation Analysis.

Abstract. *Cruciform columns have been used in several engineering applications, being known for their low torsional stiffness, which leads to strong torsional-flexural modal coupling. Three-dimensional motions of an inextensible cruciform column with low torsional stiffness, subjected to a concentrated axial load and a lateral harmonic excitation, are studied in this paper. Special attention is given to the effect of the axial load on the frequency-amplitude relation and its influence on the bifurcations and instabilities of the column, a problem not tackled in the previous literature on this subject. To this aim, the nonlinear integro-differential equations describing the flexural-flexural-torsional couplings of the column are used, together with the Galerkin method, to obtain a set of discretized equations of motion, which are in turn numerically integration using the Runge-Kutta method. Both inertial and geometric nonlinearities are considered in the present analysis. The results show that the axial load influences the stiffness of the column, changing its nonlinear behaviour from hardening to softening. A detailed parametric analysis, using several tools of nonlinear dynamics, unveils the complex dynamics of the column in the parametric or external resonance regions. Bifurcations leading to multiple coexisting solutions and chaotic motion are observed.*

1 INTRODUCTION

Slender bar elements, such as beam-column structures, can be found in several engineering applications, e.g., self-supporting towers, masts of cable-stayed towers, antennas, pipes, chimneys, micro or nano beams, risers used in offshore industry, robot arms, spacecraft stations, cranes, etc.

The stability of slender cruciform beam-columns under static loads or lateral harmonic excitations has been a frequent research topic due to its low torsional stiffness and the dangerous flexural-torsional coupling. Considering columns under static loads, one of the first studies on this topic was conducted by Hutchinson and Budiansky [1]. Recently, Schurig and Bertram [2] also studied the torsional stability of cruciform columns under compressive loads and their design was discussed by Trahair [3], among others. Crespo da Silva and Glynn [4, 5] proposed a mathematical model to study the flexural-torsional oscillations of slender beams and investigated their behaviour under uniformly distributed lateral harmonic excitation. A review of the main contributions to this topic up to 2004 can be found in the book by Nayfeh and Pai [6]. Examples of more recent research on the dynamics of free-clamped beams under lateral harmonic excitation can be found in [7].

But even today, little is known about the nonlinear vibrations and dynamic stability of cruciform columns. These columns can, when excited, exhibit large displacements, as well as nonplanar motions, leading to various types of bifurcations and coexistence of different solutions, causing sudden changes in the stress and strain states of the structure. So, our aim here is, by using tools of nonlinear dynamics, to study the three-dimensional motions and instabilities of a clamped-free inextensible cruciform column under axial loads and/or lateral harmonic excitation, with emphasis on the influence of the load on the linear frequency spectrum, nonlinear frequency-amplitude relation and dynamic bifurcations. For this the equations of motion proposed in [4,5], which includes both geometric and inertial nonlinearities, are adopted.

2 DYNAMIC SYSTEM

A uniform, homogeneous, inextensible and initially straight column of isotropic linear elastic material, length L and mass per unit length m is considered in this paper. A deformed column segment of arc length s is shown in Fig. 1, where the axes X, Y and Z define the inertial rectangular coordinate system, while ξ, η and ζ denote a local orthogonal curvilinear coordinate system of the column at arc length s in the deformed configuration, which coincides with the principal axes of the column cross section. In the undeformed configuration, the ξ and X axes are coincident and the η and ζ axes are parallel to Y and Z, respectively.

To investigate the relative influence of an axial load on the nonlinear dynamic behaviour of slender cantilever columns, a column with constant cruciform cross section with height h, width b and wall thickness e is adopted, as shown in Fig. 1. The column is subjected to an axial static concentrated load applied at the free end of the column and given by Q_u. In the Y direction a uniformly distributed lateral harmonic excitation defined by $Q_v(t) = q_v \cos(\Omega t)$ is considered, where q_v is the excitation magnitude, Ω the excitation frequency and t is time.

3 EQUATIONS OF MOTION

Using only one mode approximation for displacements in the Galerkin`s procedure, the following third-order dimensionless PDEs equations of motion are obtained:

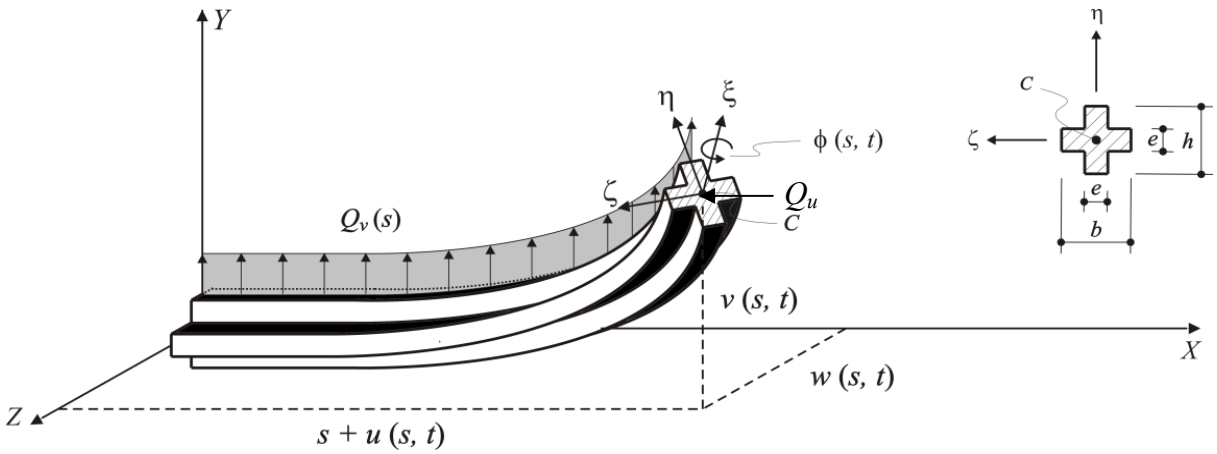

Figure 1: Coordinate systems, displacements, loads and column cross section.

$$\left[\int_0^1 F_v^2 ds - J_\zeta \int_0^1 F_v'' F_v ds\right]\ddot{v} + \left[c_v \int_0^1 F_v^2 ds\right]\dot{v} + \left[\beta_y \int_0^1 F_v^{IV} F_v ds + \int_0^1 Q_u F_v F_v'' ds\right] v = \alpha_{v1}\gamma w + \alpha_{v2} v \gamma^2 + \alpha_{v3} v w^2 + \alpha_{v4} v^3 + \alpha_{v5}\left(v^2\right)^{\bullet\bullet} v + \alpha_{v6}\left(w^2\right)^{\bullet\bullet} v + \alpha_{v7} v^2 \ddot{v} + \alpha_{v8} v w \ddot{w} + \alpha_{v9} \dot{w}\dot{\gamma} + \alpha_{v10} w \dot{v} \dot{w} + \alpha_{v11} v \left(\dot{w}\right)^2 + \alpha_{v12}\left(\dot{v}\gamma^2\right)^{\bullet} + \alpha_{v13}\gamma \ddot{w} + \alpha_{v14} v \left(\dot{v}\right)^2 + \alpha_{v15} w \dot{\gamma} + \int_0^1 F_v q_v \cos(\Omega t) ds \,, \tag{1}$$

$$\left[\int_0^1 F_w^2 ds - J_\eta \int_0^1 F_w'' F_w ds\right]\ddot{w} + \left[c_w \int_0^1 F_w^2 ds\right]\dot{w} + \left[\beta_y \int_0^1 F_w^{IV} F_w ds + \int_0^1 Q_u F_w F_w'' ds\right] w = \alpha_{w1}\gamma v + \alpha_{w2} w \gamma^2 + \alpha_{w3} w v^2 + \alpha_{w4} w^3 + \alpha_{w5}\left(w^2\right)^{\bullet\bullet} w + \alpha_{w6}\left(v^2\right)^{\bullet\bullet} w + \alpha_{w7} w^2 \ddot{w} + \alpha_{w8} w v \ddot{v} + \alpha_{w9} \dot{v}\dot{\gamma} + \alpha_{w10} v \dot{w} \dot{v} + \alpha_{w11} w \left(\dot{v}\right)^2 + \alpha_{w12}\left(\dot{w}\gamma^2\right)^{\bullet} + \alpha_{w13}\gamma \ddot{v} + \alpha_{w14} w \left(\dot{w}\right)^2 \,, \tag{2}$$

$$\left[\int_0^1 F_\gamma^2 ds\right]\ddot{\gamma} + \left[c_\gamma \int_0^1 F_\gamma^2 ds\right]\dot{\gamma} - \left[\beta_\gamma \int_0^1 F_\gamma'' F_\gamma ds\right]\gamma = \alpha_{\gamma1}\gamma v^2 + \alpha_{\gamma2}\gamma w^2 + \alpha_{\gamma3} v w + \left[\left[\alpha_{\gamma4}(v w)^{\bullet} + \alpha_{\gamma5} v \dot{w}\right]^{\bullet} + \alpha_{\gamma6}\gamma \dot{v} + \alpha_{\gamma7}\gamma \dot{w} + \alpha_{\gamma8} \dot{v} \dot{w}\right. . \tag{3}$$

Details of this formulation can be found in [8], where $v = v\,(t)$ and $w = w\,(t)$ are the deflections of the column in the Y and Z directions, respectively, and $\gamma = \gamma\,(t)$ is the angle of torsion.

Here β_y and β_γ are the non-dimensional stiffness parameters, c_v, c_w and c_γ, are the linear viscous damping coefficients, the superscript (') denotes partial differentiation with respect to s and the superscript ($\dot{}$), differentiation with respect to time t. Finally, the eigenfunctions $F_v(s)$, $F_w(s)$ and $F_\gamma(s)$ used to approximate de displacement field are given by:

$$F_{v,w} = C_{v,w}\left\{\cosh\left(r_{1,3}\, s\right) - \cos\left(r_{2,4}\, s\right) - K_{v,w}\left[\sinh\left(r_{1,3}\, s\right) - \left(r_{1,3}/r_{2,4}\right)\sin\left(r_{2,4}\, s\right)\right]\right\}, \tag{4}$$

$$F_\gamma = C_\gamma \sin\left[\left(2n-1\right)\left(\pi/2\right)s\right] \qquad \left(n = 1, 2, \ldots\right). \tag{5}$$

In the Eqs. (4) and (5), C_v, C_w and C_γ are the normalized modal amplitudes in each degree of freedom. The quantities r_1 to r_4 are obtained from the solution of the following characteristic equation:

$$r_{1,3}^4 + r_{2,4}^4 + 2\, r_{1,3}^2\, r_{2,4}^2 \cosh\left(r_{1,3}\right)\cos\left(r_{2,4}\right) + r_{1,3}\, r_{2,4}\left(r_{2,4}^2 - r_{1,3}^2\right)\sinh\left(r_{1,3}\right)\sin\left(r_{2,4}\right) = 0\,, \tag{6}$$

were the quantities r_1 to r_4 are:

$$r_1 = \sqrt{-\frac{J_\zeta\, \omega_v^2}{2\,\beta_y} + \sqrt{\left(\frac{J_\zeta\, \omega_v^2}{2\,\beta_y}\right)^2 + \frac{\omega_v^2}{\beta_y}}}\,, \tag{7}$$

$$r_2 = \sqrt{+\frac{J_\zeta\, \omega_v^2}{2\,\beta_y} + \sqrt{\left(\frac{J_\zeta\, \omega_v^2}{2\,\beta_y}\right)^2 + \frac{\omega_v^2}{\beta_y}}}\,, \tag{8}$$

$$r_3 = \sqrt{-\frac{J_\eta\, \omega_w^2}{2} + \sqrt{\left(\frac{J_\eta\, \omega_w^2}{2}\right)^2 + \omega_w^2}}\,, \tag{9}$$

$$r_4 = \sqrt{+\frac{J_\eta\, \omega_w^2}{2} + \sqrt{\left(\frac{J_\eta\, \omega_w^2}{2}\right)^2 + \omega_w^2}}\,, \tag{10}$$

and K_v and K_w, by:

$$K_{v,w} = \frac{r_{1,3}^2 \cosh\left(r_{1,3}\right) + r_{2,4}^2 \cos\left(r_{2,4}\right)}{r_{1,3}^2 \sinh\left(r_{1,3}\right) + r_{1,3}\, r_{2,4} \sin\left(r_{2,4}\right)}\,. \tag{11}$$

The flexural frequencies ω_v and ω_w can be obtained from Eq. (4) while the torsional frequencies ω_γ is given by:

$$\omega_\gamma = \left(2n-1\right)\left(\frac{\pi}{2}\right)\sqrt{\frac{\beta_\gamma}{J_\xi}} \qquad \left(n = 1, 2, \ldots\right). \tag{12}$$

In the above equations α_{vi}, α_{wi} e $\alpha_{\gamma i}$ (for i = 1, 2, 3, …) are the Galerkin's coefficients and can be found explicitly in [8].

4 NUMERICAL RESULTS

For the numerical analysis, a column with $L = 25\,b$, distributed moments of inertia $J_\eta = J_\zeta = 6.8978\text{E-}5$ and $J_\xi = 1.3796.\text{E-}4$, stiffness parameters $\beta_v = 1.0$ and $\beta_\gamma = 6.9123\text{E-}4$, and normalized modal amplitudes $C_v = C_w = 1.0$ and $C_\gamma = 1.4142$ is adopted.

In the Sec. 4.1, considering only the uniformly lateral harmonic excitation, the influence of the column cross sections geometry is studied by varying its wall thickness e and keeping the relation $h / b = 1.0$ constant (see Fig. 1). In Sec. 4.2 the frequency-amplitude relation for a column with wall thickness $e = 0.0687$ is obtained, considering only the axial static load Q_u. Finally, in Sec 4.3, the influence of the axial static load on the resonance curve is studied considering both the static load, Q_u, and a lateral harmonic excitation, $Q_v\,(s) = q_v\,cos(\Omega\,t)$.

4.1 Influence of the cross section geometry on dynamic behaviour of the column.

Table 1 the three lowest natural frequencies associated with each vibration mode for increasing values of the cross section wall thickness. As shown in Tab.1, the second and third frequencies are much higher than the first one. So a one mode approximation for each degree of freedom can be used in the Galerkin procedure to study the nonlinear dynamics of the column in the main resonance region (see Sec. 3). The two flexural frequencies are equal due to the cross section symmetry.

Case	Size	1th Frequency		2nd Frequency		3rd Frequency	
	e / b	$\omega_v = \omega_w$	ω_γ	$\omega_v = \omega_w$	ω_γ	$\omega_v = \omega_w$	ω_γ
1	0.0100	3.516	0.237	22.034	0.712	61.700	1.187
2	0.0333	3.516	1.444	22.034	4.333	61.700	7.221
3	0.0526	3.516	2.863	22.034	8.588	61.700	14.314
4	0.0556	3.516	3.104	22.034	9.312	61.700	15.520
5	0.0588	3.516	3.381	22.034	10.143	61.700	16.906
6	0.0597	3.516	3.457	22.034	10.371	61.700	17.285
7	0.0601	3.516	3.488	22.034	10.464	61.700	17.440
8	0.0602	3.516	3.504	22.034	10.511	61.700	17.519
9	0.0603	3.516	3.516	22.034	10.548	61.700	17.581
10	0.0604	3.516	3.520	22.034	10.559	61.700	17.598
11	0.0687	3.516	4.267	22.034	12.801	61.700	21.335
12	0.0769	3.516	5.049	22.034	15.147	61.700	25.245

Table 1: Cruciform cross sections investigated and natural frequencies for each case (h/b=1).

When the wall thickness e of the cross section increases, the moments of inertia J_η and J_ζ, as well as the mass of the column increases. However in the range of e/b adopted here, the frequencies associated with the flexural modes (ω_v and ω_w) are kept practically constant while the torsional frequency (ω_γ) increases with the wall thickness e. In the Tab. 1, when $e = 0.01\,b$ (Case 1), the torsional frequency is almost zero. When $0.0602 < e/b < 0.0604$, the lowest natural frequency associated with the torsional vibration mode is equal or close to the flexural modes, i.e., between Cases 8 and 9. In these cases, a complex behaviour is expected due to the 1:1:1 internal resonance. From Case 10 onwards, the torsional frequency is bigger than the flexural frequencies, decreasing its effect on the dynamics behaviour of the system.

For the forced vibration, a lateral harmonic excitation with magnitude $q_v = 0.2$ is adopted. The linear viscous damping are $c_v = c_w = c_\gamma = 5\%$. Figures 2 and 3 show, for the twelve cases listed in Tab. 1, projections of the bifurcation diagram onto the v vs. w vs. Ω and v vs. w vs. γ spaces, respectively. The continuation software AUTO [9] is used to obtain these bifurcation diagrams.

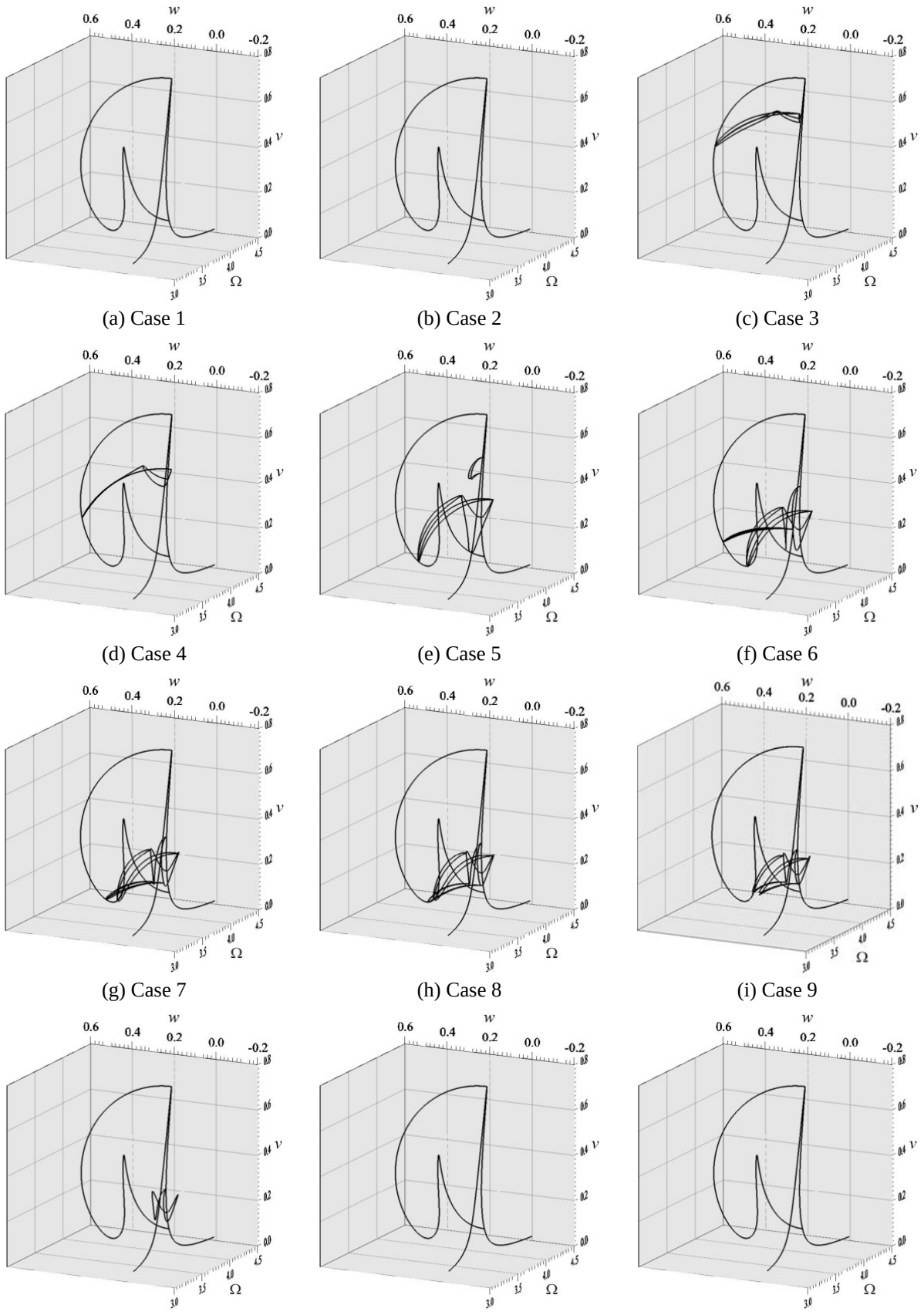

(a) Case 1 (b) Case 2 (c) Case 3

(d) Case 4 (e) Case 5 (f) Case 6

(g) Case 7 (h) Case 8 (i) Case 9

(j) Case 10 (k) Case 11 (l) Case 12

Figure 2: Bifurcation diagrams in the *v* vs. *w* vs. Ω space, for the twelve cases listed in Tab. 1.

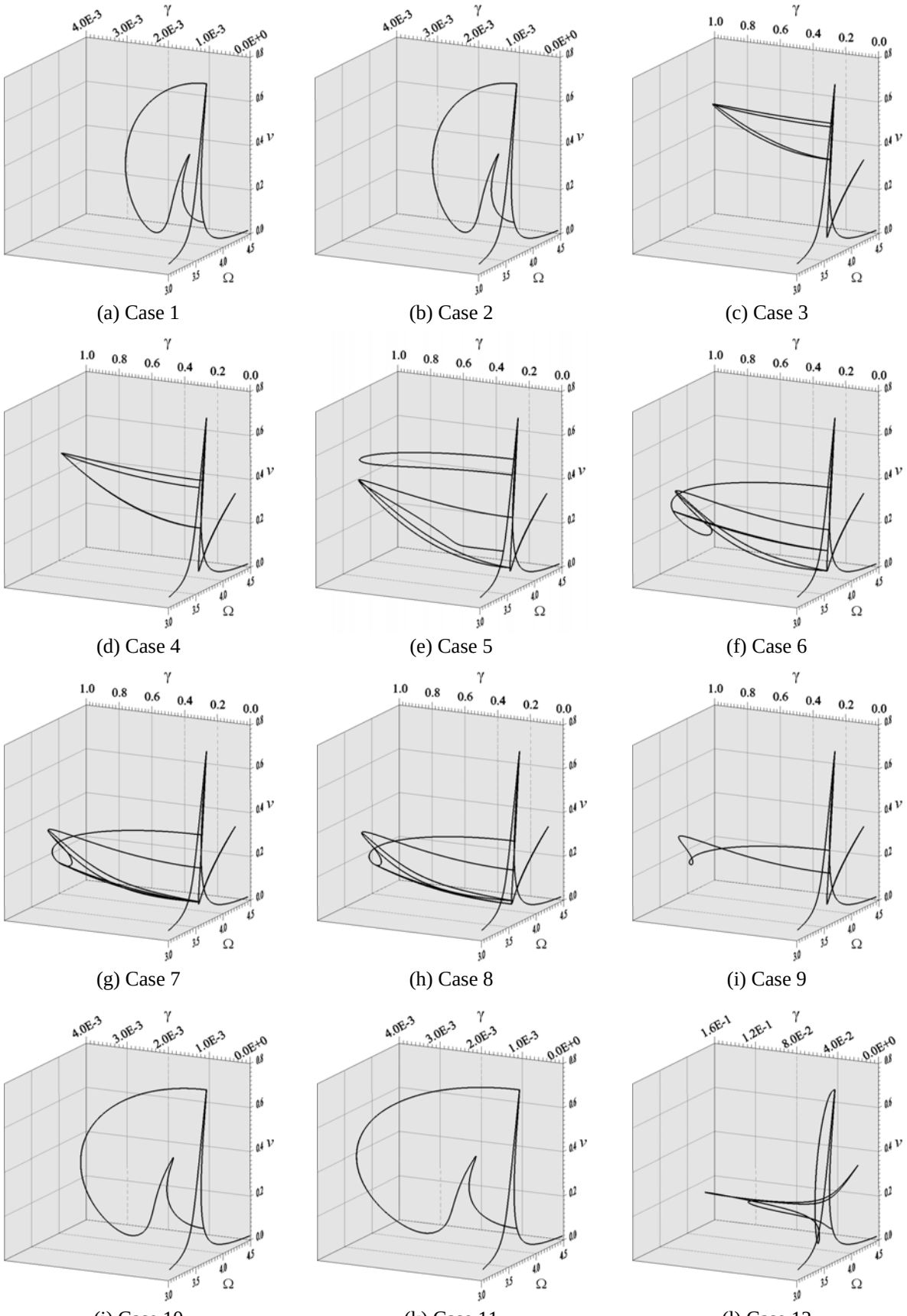

(a) Case 1 (b) Case 2 (c) Case 3

(d) Case 4 (e) Case 5 (f) Case 6

(g) Case 7 (h) Case 8 (i) Case 9

(j) Case 10 (k) Case 11 (l) Case 12

Figure 3: Bifurcation diagrams in the v vs. w vs. γ space, for the twelve cases listed in Tab. 1.

For convenience, in the Fig. 2 and 3, information on the stability of the equilibrium paths and the position of bifurcation points were omitted. These projections show a continuum variation of the bifurcation diagrams as the wall thickness increases. Even so, some important differences can be observed by comparing Cases (2-3), (4-5), (9-10) and (10-11), were, respectively, some solution branches appear, negative displacements appear in w, some solution braches disappear and the negative displacements disappear. In addition, Tab. 2 show the maximum angle of torsion attained at each bifurcation diagram of the Fig. 3. As shown in Tab. 2, the most important participation of the angle of torsion on the dynamic behavior of the column occurs near to the 1:1:1 internal resonance region.

Case	Angle of torsion γ
1	0.001877
2	0.001958
3	0.742970
4	0.883529
5	0.974443
6	0.973016
7	0.965171
8	0.960027
9	0.949435
10	0.002971
11	0.003879
12	0.130523

Table 2: Maximum angle of torsion in the bifurcation diagrams shown in Fig. 3.

4.2 Influence of the static axial load on the frequency-amplitude relation

Here, a column with sizes h / b = 1.0 and wall tackiness e/b = 0.0687 (Case 11 in Tab. 1) is adopted. First, for the undamped column is considered ($c_v = c_w = c_\gamma = 0.0$ and $Q_u = 0.0$). As shown in Tab. 1, in this case the lowest natural frequencies of the unloaded clamped-free column are $\omega_{0v} = \omega_{0w} = 3.516$ and $\omega_{0\gamma} = 4.267$. Fig. 4a shows that as the axial load increases the square of the natural frequency decreases linearly, becoming zero when the static axial load reaches its critical value, $P_{cr} = (\pi^2\, EI / 4L^2)$.

In addition, Fig. 4b illustrates the influence of the static axial load on the nonlinear frequency-amplitude relation. The unloaded column (curve 0) exhibits a small degree of geometric nonlinearity with hardening behaviour. As the axial load increases, the degree of geometric nonlinearity decreases, but the importance of inertial nonlinearities in the equations of motion increases. At a certain load level, the curve starts to bend to left. For high load levels, it exhibits a strong softening behaviour. The described behavior is typical of bar structures, where geometric nonlinearities lead to increasing effective stiffness, while inertial nonlinearities lead to a loss of stiffness, as shown in [7].

4.3 Nonlinear response of the column under static preload and lateral excitation

Now, the influence of static axial preload on the dynamic nonlinear behaviour of the column is investigated. A uniformly distributed lateral harmonic excitation, given by $Q_v\,(s) = 0.025\, cos(\Omega\, t)$, at the primary resonance region $\Omega = \omega_{0v} = \omega_{0w}$, is considerate applied in the Y direction (see Fig. 1). Fig. 5 shows two projections of the resonance curves considering $Q_u / P_{cr} = 0.0$ and $Q_u / P_{cr} = 0.15$. The continuation software AUTO [9] is used in Fig. 5a and brute force algorithm in Fig. 5b.

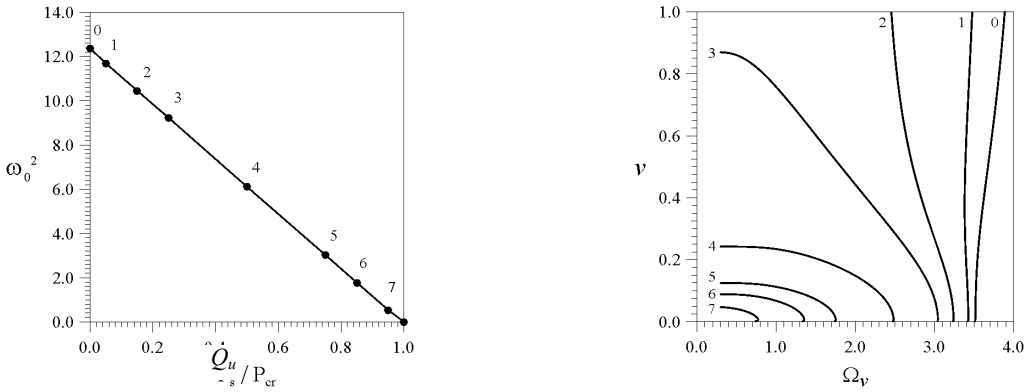

(a) Axial load vs. square frequency relation. (b) Frequency vs. amplitude relation.

Figure 4: Influence of axial load on the lowest natural frequency and frequency vs. amplitude relation.

The Fig. 5a is a 2D projection (v vs. Ω) of the Fig. 2k (without axial load), were solid lines represent stable solutions and dashed lines denotes unstable solutions. Near to the 1:1 external resonance region up to three different stable solution branches coexist, but as the static load increases, the natural frequency of the structure decreases (Fig. 4) and the resonance region moves to the left, approaching to zero, and most stable solution branches observed in the Fig. 5a become unstable, as shown in Fig. 5b for $Q_u / P_{cr} = 0.15$.

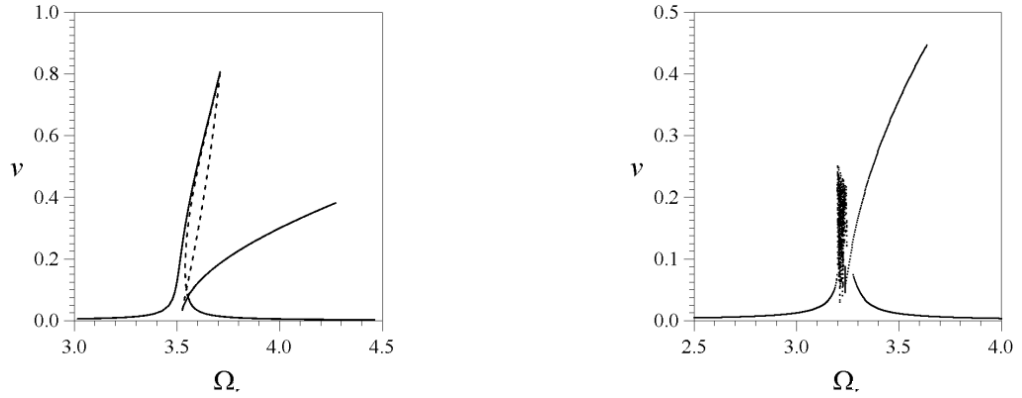

(a) $Q_u / P_{cr} = 0.0$. (b) $Q_u / P_{cr} = 0.15$.

Figure 5: Influence of static preload on the resonance curves of the column under lateral harmonic excitation.

More specifically, for this load level, a frequency range without stable periodic solutions can be observed (cloud of points) near the 1:1 external resonance region. Fig. 6 shows a time histories together with the evolution of the Lyapunov's exponents (λi, for $i = 1, 2, ..., 6$) at $\Omega = 3.20$. As shown in the Fig. 6b, at least one of the exponent is positive ($\lambda i > 0.0$), characterizing the motion of the column in this region as a chaotic.

5 CONCLUSIONS

The flexural-flexural-torsional response of a cruciform column with low torsional stiffness was investigated in this work. By using bifurcation diagrams and varying the wall thickness of the column cross section column a parametric study was carried out. The most complex dynamic behaviour occurs near the 1:1:1internal resonance region, where torsional motions become particularly important. The axial static preload has a profound influence on the fre-

quency-amplitude relation and on the resonance curves of the beam under lateral harmonic excitation. Multiplicity of solutions is observed as well as regions with chaotic motions.

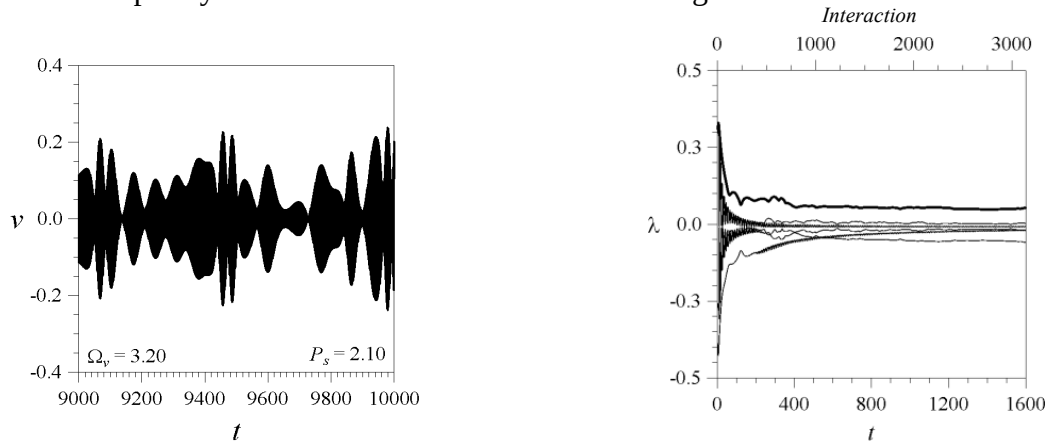

(a) Time history v vs. t. (b) Lyapunov exponents.

Figure 6: Characteristic chaotic response of the preloaded column. $Q_u / P_{cr} = 0.15$, $q_v = 0.025$ and $\Omega = 3.20$.

6 ACKNOWLEDGMENTS

The authors gratefully acknowledge the financial support of the Brazilian Research Agencies FAPERJ, CAPES and CNPq.

REFERENCES

[1] Hutchinson, J., Budiansky, B., Analytical and numerical study of the effects of initial imperfections on the inelastic buckling of a cruciform column. In: Budiansky, B. (Ed.), *Proceeding of IUTAM Symposium on Buckling of Structures*. Springer: 98–105, 1976.

[2] Schurig, M., Bertram, A., The torsional buckling of a cruciform column under compressive load with a vertex plasticity model. *International Journal of Solids and Structures*, **48**, 1–11, 2011.

[3] Trahair, N. S., Strength design of cruciform steel columns. *Engineering Structures*, **35**, 307–313, 2012.

[4] Crespo da Silva, M. R. M., Glynn, C. C., Nonlinear flexural-flexural-torsional dynamics of inextensional beams. I. Equation of motion. *Journal of Structural Mechanics*, **6**, 437–448, 1978.

[5] Crespo da Silva, M. R. M., Glynn, C. C., Nonlinear flexural-flexural-torsional dynamics of inextensional beams. II. Forced motions. *Journal of Structural Mechanics*, **6**, 449–461, 1978.

[6] Nayfeh, A. H., Pai, P. F., *Linear and nonlinear structural mechanics*. Wiley-VCH, 2004.

[7] Carvalho, E.C., Gonçalves, P.B, Rega, G., Del Prado, Z.J.G.N., Influence of axial loads on the nonplanar vibrations of cantilever beams. *AIP Conf. Proc*, **1493**, 215–222, 2012.

[8] Carvalho, E. C., Nonlinear and Nonplanar vibrations and dynamic instability of slender bars. *D.Sc. Thesis*, PUC-Rio, Rio de Janeiro, Brazil, 2013.

[9] Doedel, E. J., Champneys, A. R., Fairgrieve, T. F., Kuznetsov, Y. A., Sandstede B., Wang X. *AUTO 97*. Concordia University, Montreal, Canada, 1998.